Egypt. J. Chem. Vol. **68**, No.2, pp. 333 -347 (2025)

Egyptian Journal of Chemistry

http://ejchem.journals.ekb.eg/

Electrochemical-Based Eeg Brain Signal Recognition Using Deep Neural Networks

Sameh Attia,[a] Mohammad Sammany,[b] Ayman Haggag,[c] Tamer Nassef [d]

[a,c]Electronics Technology Department, Faculty of Technology and Education, Helwan University, 30 Elsawah St., Elamiriya, P.O. Box 11813, Cairo, Egypt

[b]Pharmacy Practice Department, Faculty of Pharmacy, Helioplis University for Sustainable Development, 3 Cairo,Belbes Desert Road P.O.Box 2834, Cairo, Egypt

[d]Computer and Software Engineering Department, Faculty of Engineering, Misr University for Science and Technology, 1 Soad Kafafi St., Al-Mutamayez District PO Box: 77 6th of October City, Giza, Egypt

Abstract

The pivotal role of electrochemistry in biologically relevant systems is underscored by its ability to elucidate the chemical interactions occurring in neural networks of the brain. This has been significantly enhanced by advancements in electrochemical principles, spurred by the mid-20th-century technological revolution. Recent advancements in electrochemical methodologies have broadened their applications from mere measurement of neurochemical levels to encompassing modulation and simulation of brain signals, as well as monitoring neuronal electrochemical activities. This progress paves the way for the application of implantable cerebral devices in the human brain. In this paper, we present the use of a Deep Neural Network (DNN), a powerful AI technique with numerous medical applications, including real-time monitoring systems for continuous evaluation of patients' emotional and neurological states. The DNN was trained to recognize three distinct types of electrochemical signals derived from Electroencephalograph (EEG) measurements using an electrode array. The model successfully identified three classes of signals corresponding to the emotional states of sadness, happiness, and neutrality in a group of volunteers subjected to various psychological stimuli. The obtained results demonstrate an exceptional classification accuracy of 98.4% on the SEED database with a minimal array of sensors applied to the brain cortex, which serve as inputs for the artificial neural network. Outperforming recent studies, which reported lower accuracies, our findings highlight the potential of our approach for practical applications in emotion recognition and related fields.

Keywords: Electrochemistry, EEG Electroencephalograph, Deep Neural Network (DNN), SEED Database;

1. Introduction

The human brain composed of sophisticated intelligent network of billions of neurons stands as the peak of natural evolution. At its core, it operates through the intricate exchange of electrical and chemical signals transductions at synaptic junctions between neurons, constituting countless neural connections and circuits that shape the multimodal brain functions [1]. This intricate network, driven by electrochemical signal, forms the basis of our understanding of neural circuits and their contribution to the brain's multifaceted functionalities. Historical advancements, notably the patch-clamp technique's introduction [2,3], have significantly propelled our comprehension of neurochemical activities within the living brain, enabling precise monitoring and modulation. These methodological innovations, together with the advent of Brain-Machine Interface (BMI) technologies and the integration of artificial intelligence (AI), signal the dawn of a transformative era in neuroscience [4]. They promise a future where the intricate neural networks can be fully delineated and manipulated, offering deeper insights into the brain's chemical and electrical intricacies.

The exploration into the brain's chemical landscape aims to elucidate the fundamental processes governing neural activity, with a focus on the critical role of neurotransmitters such as dopamine, serotonin, and glutamate [5]. These chemical messengers, essential for transmitting signals across synaptic gaps, play pivotal roles in mood regulation, cognition, and sensory perception [6]. A notable pathway in this complex chemical tapestry is the synthesis of serotonin from tryptophan, which undergoes hydroxylation to 5-Hydroxytryptophan (5-HTP) and subsequent decarboxylation to serotonin [7,8]:

$$C_{11}H_{12}N_2O_2+O_2 \rightarrow C_{11}H_{12}N_2O_3+H_2O \; C_{11}H_{12}N_2O_3 \rightarrow C_{10}H_{12}N_2O+CO_2$$

Serotonin's release into the synaptic cleft and its binding to post-synaptic receptors underscore the dynamic nature of neural signaling, which underlies our thoughts, emotions, and reactions [9]. Disruptions in these pathways, like serotonin imbalances, have been linked to mood disorders, emphasizing the crucial role of chemical interactions in mental health [10].

*Corresponding author e-mail: Sameh.driaspost21@techedu.helwan.edu.eg , (Sameh Attia)

Receive Date: 21 May 2024, Revise Date: 26 June 2024, Accept Date: 03 July 2024

DOI: 10.21608/ejchem.2024.291437.9748

Neurons communicate with each other through synaptic transmission, where neurotransmitters are released and received by neighboring neurons. This process involves complex electrochemical changes, including the movement of ions like sodium, potassium, and calcium across neuronal membranes [11]. These ion movements lead to the generation of small electrical potentials, such as postsynaptic potentials and action potentials. When a large number of neurons are active simultaneously and their activity is synchronized, these potentials sum up to generate measurable electrical fields [12]. EEG is a primarily techniques to measures the electrical activity of the brain, which indirectly reflects the underlying electrochemical processes. It captures the electrical fields generated by the ionic current flows within the brain's neurons [13]. EEG electrodes placed on the scalp detect these summed electrical fields, where the signals picked up by EEG represent the averaged activity [14]. This endeavor not only offers insight into the brain's fundamental operations but also opens pathways for developing targeted pharmacological interventions, providing hope for individuals with mental health disorders and marking a significant stride to decipher the brain's electrochemical mysteries [15]. Brain–Computer Interface (BCI) directly connects human brain activity with artificial effectors, which provides an interactive pathway between the human brain and external devices for various applications [16]. The process of such an interaction begins with the capture of brain activity through the signal processing and analysis to detect the users' intent. BCI systems, along with their diverse applications, have been the focus of extensive research over many years. Emotion recognition emerges as a particularly intriguing area of study due to its wide range of potential applications across various scenarios [17]. EEG signals are recognized as a reliable marker for significant mood alterations in humans. Thus, it has been widely used for research into emotion recognition [18].

In recent years, researchers in the fields of emotional computing have been working on emotional expression analysis based on visual and physical signals. The most common signs include neurophysiological signals that highly subjective and their information can be artificially hidden from accurate judgment [19,20,21,22]. However, physical signals can provide more accurate and objective emotional recognition in real-time responses exhibiting greater sensitivity to mood variations compared to peripheral signals [23]. In fact, EEG patterns of emotional activities are relatively stable over time [24]. However, the collected EEG signal is non-stationary and often mixed with a large amount of noise, resulting in a low signal-to-noise ratio [25]. Therefore, emotional recognition based on EEG signal has some difficulties [23]. If the amount of data is insufficient, the features automatically extracted by deep models are not as discriminative as manually designed features based on neuroscience knowledge. Therefore, some researchers have attempted to combine manually designed features in in deep models to identify emotions more accurately [26]. Atkinson and Campos [27] and Kumar et al. [28] performed on the DEAP database. While Kumar et al. used just two EEG electrodes to calculate the bispectrum feature for theta, alpha, and beta frequency bands using HOSA, Atkinson et al. used 14 EEG electrodes to calculate band power, the Hjorth parameter, fractal dimension, and some statistical parameters like median, standard deviation, and kurtosis coefficients. The minimum redundancy maximum relevance (mRMR) method was utilized for feature selection in the context of extensive feature extraction. In classification, a combination of genetic algorithm with SVM (GA-SVM) was constructed to classify three different emotions with average accuracy of approximately 61.51%. SVM was implemented to classify four emotions with the average accuracy of 63.01%. Wang et al. [29] used three different databases, including USTC-ERVS, DEAP, and MAHNOB-HCI for evaluation purpose. A substantial set of EEG electrodes and other peripheral signals were chosen; the power spectrum derived from EEG channels was computed and merged with features from peripheral signals in a novel combination. Stikic et al. [30] measured 20 EEG electrodes using wireless sensor headset, and calculated two extraction features of PSD and wavelets. Both Linear Discriminant Function Analysis (LDFA) and Quadratic Discriminant Function Analysis (QDFA) were tested to classify positive and negative emotions, and achieved high accuracy of approximately 94.5%. Nasehi and Pourghassem [31] applied Gabor function to extract spectral, spatial, and temporal features for EEG brain channels. RF classifier with T7 channel produced the best average accuracy of approximately 93.46% and 80.53% for SEED and DEAP database, respectively [32]. Cimtay et al. [33] used a convolutional neural network (CNN) to extract the spatial features of emotional activities, and accuracies of 86.56% and 72.81% were achieved on the SEED and DEAP datasets, respectively. Wang et al. extended the dimension of CNN and designed EmotioNet to obtain spatial features [34]. The accuracy of 15 subjects is above 90%, and the average ACC and STD of emotion classification are 97.20% and 1.57%, respectively [26] and 76% for the SEED-IV dataset [35]. The systematic review paper [36], and the emotion recognition survey paper [37] reveal that this topic still faces additional challenges [38].

In this article, an emotion classification system is proposed based on the frequency-time analysis of EEG brain signals taken from SEED emotional stimuli databases for a group of volunteers subjected to various psychological stimuli. A DNN was trained to recognize three distinct types of electrochemical signals corresponding to the emotional states of sadness, happiness, and neutrality. The obtained results demonstrate an exceptional classification accuracy of 98.4% on the SEED database with a minimal array of sensors applied to the brain cortex, which serve as inputs for the artificial neural network. The subsequent sections of this document are structured as follows: Section 2 delves into Brain Chemistry, detailing the interactions of neurotransmitters and their influence on neural activity. Section 3 focuses on Electrochemical-Based EEG Signals, discussing how EEG captures these electrochemical interactions. Section 4 covers the Materials and Methods, including the Emotional EEG Datasets in Section 4.1, the architecture of Deep Neural Networks in Section 4.2, and the role of The Adam Optimizer in Section 4.3. Section 5 presents the Experimental Setup and Results, highlighting the performance metrics of the proposed model. Section 6 provides a comprehensive Discussion, comparing the results with existing research and exploring the implications of our findings. Finally, Section 7 concludes the paper, summarizing the key contributions and suggesting directions for future work.

2. Brain Chemistry

The electrochemical processes in the brain, particularly those involved in neuronal communication, are governed by a series of complex chemical reactions and ion exchanges [39]. Neurons maintain a resting membrane potential primarily through the differential distribution of ions, especially sodium (Na^+) and potassium (K^+), across their membranes, facilitated by Na^+/K^+-ATPase Pump Action:

$ATP + 3Na^+(in) + 2K^+(out) \xrightarrow{Na^+/K^+\text{-ATPase}} ADP + Pi + 3Na^+(out) + 2K^+(in)$ Neurotransmitter Release (e.g. Glutamate):

$Ca^{2+}(in)$ +Vesicle $[Glutamate] \xrightarrow{Fusion}$ Released Glutamate+Vesicle

Post-synaptic Receptor Activation:

$Glutamate + Receptor \xrightarrow{Binding} Receptor\text{-}Glutamate\ Complex \xrightarrow{Na^+ influx} Response$ [40]. This pump moves ions against their concentration gradients, generating electrical potentials essential for neuron function. Action potentials, initiated by the rapid influx and efflux of sodium and potassium ions, involve voltage-gated channels responding to changes in membrane potential [41]. At the synaptic junction, neurotransmitter release is triggered by an influx of calcium ions Ca^{2+}, facilitating the fusion of vesicles with the presynaptic membrane [42]. This process leads to the release of neurotransmitters like glutamate, which bind to receptors on the post-synaptic neuron, initiating various responses such as excitatory or inhibitory postsynaptic potentials (EPSPs or IPSPs) [43]. Figure 1 depicts the action potential propagation, neurotransmitter release, and binding processes at the synaptic junction, facilitated by ionic movements through voltage-gated channels.

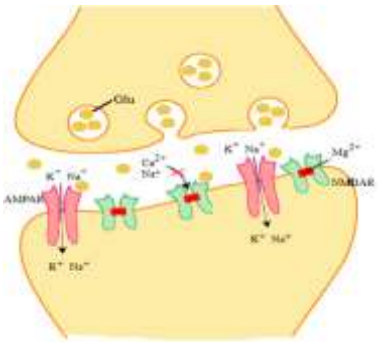

Fig. 1. Schematic diagram of synaptic transmission [44]

The exploration of the brain's complexities has been profoundly enriched by electrochemical perspectives, tracing a lineage of discovery that unveils the intricate dance of ions and molecules orchestrating neural activity. Initiated by early observations of ion flux across neuronal membranes, epitomized by the iconic Nernst equation, the field has evolved to elucidate the nuanced chemical dialogues underpinning thought and emotion [45,46]. Happiness is often associated with increased levels of neurotransmitters like serotonin, dopamine, and endorphins. While there isn't a simple "equation" for happiness, the synthesis and action of these neurotransmitters can be described in simplified reactions [47]. Serotonin Synthesis: Tryptophan to5-HTP:

$$\text{5- Hydroxytryptophan } (C_{11}H_{12}N_2O_3) \longrightarrow \text{Serotonin (5-HT, } C_{10}H_{12}N_2O) + CO_2$$

Enzyme: Tryptophan hydroxylase [48].
5-HTP to Serotonin:

$$\text{Tryptophan } (C_{11}H_{12}N_2O_2) + O_2 \longrightarrow \text{5- Hydroxytryptophan (5-HTP, } C_{11}H_{12}N_2O_3) + H_2O$$

Enzyme: Aromatic L-amino acid decarboxylase.
Dopamine Synthesis:
Tyrosine to L-DOPA:

$$\text{Tyrosine } (C_9H_{11}NO_3) + O_2 \rightarrow \text{L-DOPA } (C_9H_{11}NO_4)$$

Enzyme: Tyrosine hydroxylase [49].
L-DOPA to Dopamine:

$$\text{L-DOPA } (C_9H_{11}NO_4) \rightarrow \text{Dopamine } (C_8H_{11}NO_2) + CO_2$$

Enzyme: DOPA decarboxylaseEndorphins [50,51]. Peptides and their synthesis involve protein translation processes, which are complex and not easily represented as a simple equation. Sadness and depressive states have been linked to lower levels of serotonin and dopamine. Additionally, the stress hormone cortisol is often elevated during prolonged periods of sadness or stress [52].

Cortisol Synthesis: Cholesterol to Pregnenolone (Initial step):

$$\text{Cholesterol } (C_{21}H_{46}O) \longrightarrow \text{Pregnenolone } (C_{21}H_{32}O_2) + \text{byproducts}$$

Enzyme: CytochromeP450scc

Pregnenolone to Cortisol (Final product, simplified):

$$\text{Pregnenolone } (C_{21}H_{32}O_2) \rightarrow \text{multiple steps} \rightarrow \text{Cortisol } (C_{21}H_{30}O_5)$$

Key enzymes: 21-hydroxylase, 11β-hydroxylase [53]. This pathway involves multiple steps, with key enzymes like 21-hydroxylase and 11β-hydroxylase facilitating the conversion of precursors to cortisol in the adrenal glands. It's important to note that these descriptions vastly simplify the actual biochemical processes and the complex interplay between different systems in the brain and body. Emotional states result from dynamic changes in these chemicals, influenced by an individual's environment, perceptions, and experiences. On the development roadmap of in vivo electrochemistry, coupling of artificial intelligence (AI) is an irresistible trend. With the aid of AI technology, the range of neurochemical space that can be explored for electrochemical sensing can be significantly expanded [1].

DNNs can be trained for extracting multianalyte signatures from a convoluted signal or processing chemical and electrical signals simultaneously recorded by pixeled sensor arrays [54]. Various AI algorithms may be applied for digging out the underneath signal correlations by data mining ultimately establish chemical models for brain functions [1]. The prospect of brain research is to comprehensively chart the interactive neural networks encompassing both electrical and chemical languages that are readable and editable. While state-of-the-art BMIs heavily rely on electrophysiology, there is the chance for electrochemistry to make a splash and propel the new wave of innovations in neuroscience [1].

3. Electrochemical-Based EEG Signal

Emotion itself constitutes a psycho-physiological process or electrical brain activity pulses that reflect the states of feelings, behaviors, psychological changes, and cognition in a complex manner. The voltage fluctuation of brain neurons can be simulated using a Generic System Image (GSI), where image rows represent the frequency range, image columns represent the time pass, and the image itself is considered as a visualization map that reflects the fluctuation of the EEG voltage signal. The GSI feature extraction describes the voltage magnitude change of brain neuron in both time and frequency domains [38]. Previous works have shown that EEG contains much information about emotion, making it possible to decode emotions based on EEG signals [55,56,57,58]. Moreover, EEG is favored for its portability, affordability, and high temporal resolution, which allows it to detect subtle emotional changes. These attributes have led to its widespread application in emotion recognition [59,60,61,62]. For happy GSI images, high-intensity pixels locate several places, and exist within all frequency bands. In sad GSI images, most of high-intensity pixels do not exceed alpha frequency band (8–13 Hz). High-intensity pixels spread obviously in beta (14–30 Hz) and gamma (31–45 Hz) frequency bands for sad GSI images [38]. Among these physiological signals, EEG signals have been widely used for research into emotion recognition [63]. The flow diagram of emotion classification-based EEG brain signals is shown in figure 2 This diagram details the sequential processes from EEG data acquisition, through signal processing and feature extraction, to the final classification of emotions using a deep neural network. Each step is annotated to emphasize the integration of advanced signal processing algorithms and AI techniques, demonstrating how raw EEG data is transformed into interpretable emotional states.

4. Materials and Methods

Two conventional methods exist for categorizing human emotions: the discrete basic emotion description approach and the dimensional approach. According to the discrete basic emotion description approach, emotions can be classified into six basic emotions: sadness, joy, surprise, anger, disgust, and fear [64]. For the dimension approach, the emotions can be classified into two (valence and arousal) or three dimensions (valence, arousal, and dominance) [65]. Within these dimensions, valence indicates the degree of positivity or negativity in a person's emotions, while arousal refers to the level of excitement or apathy of emotion. Many new methods on feature extraction and classification have recently been proposed for emotion detection. For more details, we refer to the comprehensive survey outlined in [66].

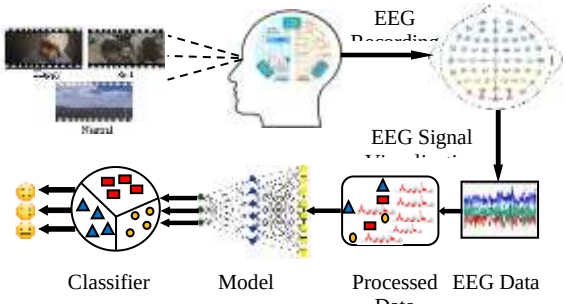

Fig. 2. EEG signal classification system flowchart

4.1. Emotional EEG Datasets

To detect abnormalities or the electrical activity of the brain, small metal electrodes with thin wires are pasted onto the human scalp. The electrodes detect electrical charges and waves that result from brain neurons activity. Then, the electrical charges are amplified and presented as a graph on a computer screen, or as a recording that may be printed out on paper [67]. Due to its direct correlation with brain cell activity, EEG has been selected for emotion detection. Additionally, its safety and cost-effectiveness make it an ideal brain testing technology [68]. From technical and feature extraction analysis, emotion classification based on EEG brain signals can be implemented using several techniques [69]. The most-common technique is time domain analysis for calculating the Hjorth parameter, fractal dimension, and signal statistical information as a mean, standard deviation, and variance. The second technique is frequency domain analysis, such as calculating power spectral density (PSD), fast Fourier transform (FFT), band power, higher-order spectrum analysis (HOSA), and relative power [70]. The primary challenges in emotion analysis using EEG are feature extraction and classifier design. Current methods predominantly employ machine learning techniques and depend on manually extracted features [23]. During the EEG recording, the international 10/20 system is used to describe the position of the electrodes on the scalp. It is based on the relation between the electrode position and the underlying area of the cerebral cortex [71]. Only one EEG channel (Fz) is needed as a data entry, without any other peripheral signals, such as heartbeats, temperature, eye movement, and blood pressure.

The middle-half-channel of EEG signal is crucial for feature extraction, significantly reducing computation and eliminating the need for feature selection methods [38]. A public dataset collected by Shanghai Jiao Tong University includes data from 15 subjects (7 males and 8 females) used for analyzing and predicting human emotion states (Zheng and Lu 2015). Data collection involved subjects watching 15 film clips, each lasting about 4 minutes, designed to be easily understood and elicit emotions effectively. The SEED dataset trials included a start hint (5 s), a movie clip (4 min), a self-assessment period (45 s), and a rest period (15 s). EEG data was gathered from 62 electrodes, more comprehensive than the DEAP dataset, and was downsampled to 200 Hz with a bandpass filter applied from 0 to 75 Hz. Additionally, to evaluate the proposed network equitably, data were filtered from 4.0 to 45.0 Hz. The dataset categorizes emotions into negative, positive, and neutral labels, with values of -1, 1, and 0, respectively. Each film clip, tailored to provoke a distinct emotion, contributes to one of three emotional categories, ensuring five clips per emotion. During these experiments, EEG signals were collected using a 62-channel system at a sampling rate of 1000 Hz [65]. Data preprocessing involved normalizing officially provided EEG signals by dividing each channel's raw signal by its maximum to standardize data distribution across input layers and converting data labels into one-hot encoding to transform categorical data into a unified digital format, aiding machine learning computations.

4.2. Deep Neural Networks

Due to the classification process, emotion classification researchers have utilized different methods, beginning with ordinary machine learning tools followed by deep learning methods [72]. Various classification methods have been used for emotion recognition, such as k-Nearest Neighbor [73] and Multi-Layer Perceptron [74]. A Support Vector Machine (SVM) and Linear Regression (LR) were used in [75], but recognition accuracy can be improved. In recent years, deep neural networks (DNN) [76] has been developed into one of the most effective and popular methods in many research fields [77,78,79,80,81]. Convolutional EEG emotion classification using the CNN method was also explored in the approaches of [76Nonetheless, the accuracy of emotion recognition achieved solely through the use of CNNs remains limited. In the work of [82], a deep learning framework consisting of the sparse autoencoder (SAE) and logistic regression was used to classify EEG emotion status. However, the reported accuracy is not high, and there are no comparative experiments to validate the results of the SAE [83]. Despite the great success of deep learning in AI applications [84,85], it suffers from a long training process and complex architecture. This is, especially, the case for large-scale data applications, in which more deep knowledge or better analysis leads to more complex design with huge dimensions [86,87]. In fact, these issues could impact sensitivity and speed-dependent applications in everyday human activities, particularly in critical real-time systems.

4.3. The Adam Optimizer

Adam stands out as a top-tier optimization algorithm in model training due to its adaptive approach to learning rates for individual parameters, ensuring efficient progress. Analogous to navigating diverse terrains, Adam dynamically adjusts its speed based on the loss landscape, speeding up in simpler areas and slowing down in complex regions to find the quickest path to minimal loss in machine learning applications. At its core, Adam's algorithm enhances gradient descent by incorporating moving averages of gradient moments, allowing intelligent learning rate adjustments for each parameter. By keeping track of unique learning rates for individual parameters and smartly adapting to data characteristics, Adam ensures efficient optimization, facilitating memory of past gradients to inform current parameter adjustments and dynamically adjusting step sizes based on gradient changes. The significance of Adam lies in its adaptive learning rates, which personalized scaling for each parameter update influences optimization efficacy, particularly in complex models. The algorithm is mathematically encapsulated in the flowing equations [88]:

$$
\begin{aligned}
g_{t} &= \nabla_{\theta} f_t(\theta_{t-1}) \\
m_t &= \beta_1 m_{t-1} + (1 - \beta_1)\, g_t \\
v_t &= \beta_2\, v_{t-1} + (1 - \beta_2) g_t^{\,2} \\
\hat{m}_t &= m_t / \left(1 - \beta_1^{\,t}\right) \\
\hat{v}_t &= v_t / \left(1 - \beta_2^{\,t}\right) \\
\theta_{t+1} &= \theta_t - \alpha\, \hat{m}_t / \left(\sqrt{\hat{v}_t} + \epsilon\right)
\end{aligned}
\qquad (1)
$$

Where:

g_t represents the gradient at iteration t
m_t is the first-moment vector at time step t
v_t is the second-moment vector at time step t
m_t is the bias-corrected first-moment estimate of gradients
v_t is the bias-corrected second-moment estimate of gradients
θ_{t+1} is the updated parameters
α is the learning rate
β_1 and β_2 are exponential decay rates
ϵ is a small scalar added for numerical stability
These equations showcase Adam's meticulous approach to parameter adjustments and adaptive learning rates, highlighting its effectiveness in optimizing complex models efficiently.

5. Experimental Setup and Results

The SEED dataset, originally comprising 8100 records with 2760 attributes across three emotional classes (positive, neutral, and negative), underwent rigorous data preprocessing regimen to prepare it for the DNN model. To provide an approximate distribution of the 2760 input features in the SEED dataset across different feature groups, we made a rough segmentation for the feature vector based on five categories used in EEG feature selection for emotion recognition as follows:
1. Time Domain Features: Assuming a modest set of 4 basic statistical features (mean, standard deviation, skewness, kurtosis) per channel, and considering EEG datasets often use 32, 64, or more channels.
2. Frequency Domain Features: including power spectral density in various bands (Delta, Theta, Alpha, Beta, Gamma). Average band power is calculated for 5 frequency bands each, (assuming 32-64 channels).
3. Time-Frequency Domain Features: More detailed features derived from wavelet transform assuming similar number of features per band as in the frequency domain, but with additional granularity.
4. Connectivity Features: Can significantly increase the feature count with a higher number of channels. A subset of these pairs is considered for 64 channels.
5. Higher-Order Features and Nonlinear Dynamics Features: This features category is less numerous but more complex. Ten features per channel are selected
including entropy measures, Hjorth parameters, and others. Table 1 and figure 3 summarize the features types and the approximate range of features count per category.
The second step involved cleaning the dataset to remove any corrupt or irrelevant data entries, ensuring the integrity of the analyses. Subsequent normalization was applied to each feature, scaling the data to a common range and reducing potential bias due to differing scales.

Table 1. EEG feature extraction categories and counts

Feature Category	Description	Count
Time Domain	Basic statistical measures	160-320
Frequency Domain	Average band power	160-320
Time-Frequency Domain	Wavelet transforms with additional granularity	320-960
Connectivity Features	Correlation between pairs of channels	500-1000
Higher-Order Features and Non-linear Dynamics Features	Entropy measures, Hjorth parameters, and others	160-640

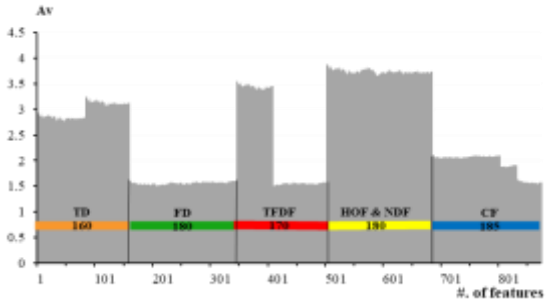

Fig. 3. The distribution of feature types across different categories

Furthermore, feature selection techniques were employed experimentally based on the previous analysis to reduce the dimensionality of the data from 2760 attributes to 875. The features were meticulously selected and ranked based on their contribution to the model's performance, ensuring a comprehensive analysis of the EEG signals. Time domain and time-

frequency domain features are typically critical for capturing essential signal characteristics, while connectivity features provide insights into the interactions between different brain regions. Higher-order features and non-linear dynamics add further depth to the analysis but may not be as consistently impactful across all models. This approach allowed the model to effectively capture and interpret the complex patterns associated with different emotional states. This reduction not only alleviates the computational burden but also enhances the model's ability to generalize by focusing on the most informative features. As demonstrated in Table 2, the prepared dataset was divided into three distinct subsets to facilitate a robust training and evaluation of the model as follows: 70% of the data, amounting to 5670 records, was used for training the model, allowing it to learn and adapt to the patterns of emotional classification, and 20% of the data, which includes 1620 records, was reserved for validation. This subset helps in tuning the model parameters and preventing over-fitting by providing a platform to assess model performance during the training phase. The remaining 10%, or 810 records, constitute the testing set used to evaluate the model's performance. This final assessment is crucial as it provides an unbiased evaluation of how well the model generalizes to new unseen data. The network was configured as depicted in figure 4, featuring a multi-layer architecture designed to effectively capture and analyze the complexities inherent in EEG data. The specifics of the learning parameters are detailed in Table 3. The model employs the Adam optimizer, known for its efficient handling of sparse gradients and adaptability. The learning rate was initially set at 0.001, with a gradient threshold of 0.9 to maintain stability in weight updates. The network was trained for up to 1000 epochs, with a mini-batch size of 50, optimizing both the learning pace and computational efficiency.

Table 2. Distribution of the SEED dataset for the emotional states

Emotion	Training		Validation		Testing		
Status	#	%	#	%	#	%	
Happy	1873	23.12	537	6.63	290	3.58	
Sad	1879	23.19	538	6.64	273	3.37	
Natural	1918	23.67	535	6.60	247	3.05	
Total	5670	70	1610	20	810	10	8100 100

The training and validation loss decreased consistently aligning with increases in accuracy, which is indicative of effective learning and model convergence. Figure 5 displays the progression of training and validation accuracy over epochs for the DNN model. The model was efficient in terms of computation, with training times due to the reduced feature set and optimized network parameters. The testing accuracy closely matched the validation accuracy, which reflects to the model's

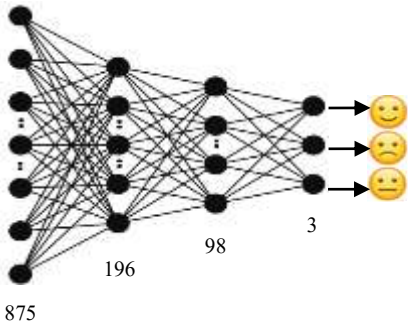

Fig. 4. DNN architecture for emotion detection

ability to generalize beyond the training data to new, unseen datasets. In the evaluation of the emotion recognition model, four key categories are essential to evaluate the model's accuracy in distinguishing between emotional states, see Table 4. Table 5 displays the classification outcomes for predicting emotional and non-emotional states, highlighting the four categories, which are essential for assessing the precision and recall of the model.

Table 3. Configuration parameters of the DNN model

Type	Parameter	Value
DNN	Optimizer	Adam
	Initial Learn Rate	0.001
	Gradient Threshold	0.9
	Learn Rate Drop Factor	0.99
	Validation Frequency	5
	Max Epochs	1000
	Mini Batch Size	50

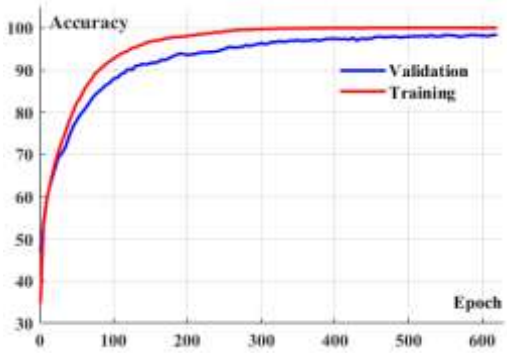

Fig. 5. Training and validation accuracy over epochs

Table 4. The essential key categories to evaluate the model's accuracy

Class	Predicted Positive	Predicted Negative
Class of Emotion (Positive)	Predicted Emotion as Emotions (TP)	Predicted Emotion as Normal (FN)
Class of Emotion (Negative)	Predicted Normal as Emotions (FP)	Predicted Normal as Normal (TN)

Table 5. Classification outcomes for predicting emotional states

Class	Predicted Positive	Predicted Negative
Class of Emotion (Positive)	553	10
Class of Emotion (Negative)	1	246

Across the different phases training, validation, and testing the model consistently achieved high accuracy levels, nearing 98.4% on the test set, indicating a well-tuned model that generalizes well across different subsets of data. Figure 6 categorizes the correct and incorrect classifications for three emotional states across training, validation, and testing phases, detailing both counts and percentages to thoroughly assess model accuracy and consistency.

For a rigorous evaluation of our model, a comprehensive account of performance metrics across three distinct data partitions—training, validation, and testing is presented in Table 7 and figure 7. A detailed explanation of each evaluation metric, illustrating it equation is provided in Table 6. This structured approach allows for a precise assessment of the model accuracy, robustness, and generalization capabilities across various emotional states. The model exhibited a sensitivity and specificity above 98%, reflecting its ability to identify positive and negative classes accurately without significant confusion. Figure 8 shows the ROC curve and AUC, which reflects our model's ability to maintain high sensitivity while minimizing the false positive rate, a testament to its precision in classifying the emotional states accurately.

Confusion Matrix			Classes						Total	
			C_1		C_2		C_3			
			#	%	#	%	#	%	#	%
Classes	C_1	Training	1873	100	0	0	0	0	**1873**	**100**
		Validating	522	97.21	1	0.19	14	2.07	**537**	**97.21**
		Testing	285	98.28	0	0	5	1.72	**290**	**98.28**
	C_2	Training	0	0	1879	100	0	0	**1879**	**100**
		Validating	7	1.3	532	97.08	9	0.17	**548**	**97.08**
		Testing	2	0.73	266	97.44	5	1.83	**273**	**97.44**
	C_3	Training	0	0	0	0	1918	100	**1918**	**100**
		Validating	2	0.37	1	0.19	532	99.41	**535**	**99.44**
		Testing	1	0.41	0	0	246	99.59	**247**	**99.59**
Total		Training	1873	100	1879	100	1918	100	**8100**	**98.4**
		Validating	522	97.21	532	97.08	532	99.41		
		Testing	285	98.29	266	97.44	246	99.59	**810**	**797**

Fig. 6. Detailed confusion matrix for multi-class emotion recognition

We note that all the experiments and analyses were conducted using MATLAB version R2023a. The implementation was carried out on a system with an Intel(R) Core(TM) i5-5200U CPU @ 2.20GHz, 8.00 GB RAM, and a 64-bit Windows 10 operating system with an x64-based processor.

6. Discussion

It is clear from the experimental results that the model's exceptional performance is evident from the detailed analysis of the classification accuracy across different emotional states using various metrics, as illustrated in Tables 5, 7 and figures 5, 6, and 7. Figure 8 includes insights from the ROC curve and AUC, which affirm the model's superior classification performance. The ROC curve demonstrates the model's capability to maintain high sensitivity without compromising specificity, a critical factor in medical and psychological applications where the accurate classification of emotional states is paramount. These elements provide a comprehensive view of the model's capabilities in emotion recognition, using artificial intelligence techniques. Figure 4 and Table 7, which present the basic architecture and the corresponding performance metrics, respectively, highlight the model's ability to achieve high accuracy levels consistently across training, validation, and testing phases. This indicates a robust model that generalizes well to new data, an essential characteristic for practical applications. Figure 5, which depicts the training and validation accuracy over epochs, shows rapid convergence of the model, suggesting that the learning rate and other hyper-parameters were well-tuned to the task. This figure underscores the computational efficiency and effective learning rate adaptation, facilitated by the Adam optimizer and other training parameters as detailed in Table 3. The advanced metrics reported in Table 6 and visualized in figure 7 demonstrate the model's precision in distinguishing between different emotional states. The high F1-Scores across all categories, combined with low FPR and FNR, reflect the model's ability to balance sensitivity and specificity effectively. Furthermore, the comparison of these results with previous works from 2019 to 2024, as summarized in Table 8, shows that the current model outperforms earlier approaches, achieving higher accuracy and robustness in emotion classification. This comparison not only validates the efficacy of the current model but also highlights the improvements made over previous methodologies. Finally, it is noteworthy to mention that the combination of an optimized DNN architecture, feature selection, diverse training data, and a rigorous evaluation process has led to the significant improvements in accuracy and robustness of the proposed model over previous approaches. These enhancements make the model highly suitable for practical applications in emotion recognition and related fields.

Table 6. Explanations and equations of each evaluation metric

Metric	Description	Equation
ACC	Accuracy	$(TP+TN)/(TP+TN+FP+FN)$
PPV	Precision and positive predictive value	$TP/(TP+FP)$
TPR	Recall, sensitivity, true positive rate, and detection rate	$TP/(TP+FN)$
FNR	Miss rate and miss false negative rate	$FN/(TP+FN)$
TNR	Specificity, selectivity, and true negative rate	$TN/(FP+TN)$
FPR	False alarm and false positive rate	$FP/(FP+TN)$
F1 Score	F1 Score and F Measure	$2(PPV\times TPR)/(PPV+TPR)$
AUC	The area under the curve or area under the ROC curve	
ROC	A graph where the x-axis and y-axis represent FPR and TPR, respectively	

Table 7. Detailed performance evaluation metrics for the proposed model across training, validation, and testing phases

			Emotion Type			
			C_1	C_2	C_3	All Classes
Metric	ACC	Training	100	100	100	100
		Validating	98.52	98.35	98.4	98.4
		Testing	99.01	98.76	98.64	98.64
	PPV	Training	100	100	100	100
		Validating	98.31	99.63	95.86	95.86
		Testing	98.96	100	96.09	96.09
	TRP	Training	100	100	100	100
		Validating	97.21	97.08	99.44	99.44
		Testing	98.28	97.44	99.6	99.6
	FNR	Training	0	0	0	0
		Validating	2.79	2.92	0.56	0.56
		Testing	1.72	2.56	0.4	0.4
	TNR	Training	100	100	100	100
		Validating	99.17	99.63	97.88	97.88
		Testing	99.42	100	98.22	98.22
	FPR	Training	0	0	0	0
		Validating	0.83	0.37	2.12	2.12
		Testing	0.58	0	1.78	1.78
	F_1Score	Training	100	100	100	100
		Validating	97.75	98.34	97.61	97.61
		Testing	98.62	98.7	97.81	97.81

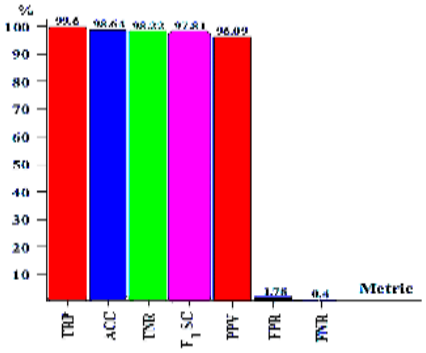

Fig. 7. The performance of the proposed model across the evaluation metrics

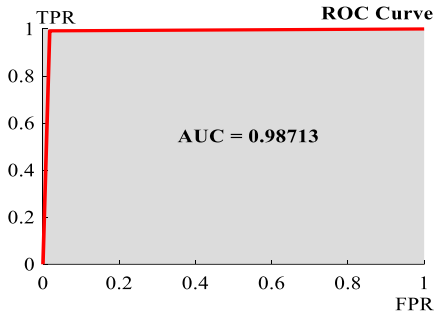

Fig. 8. Classification outcomes for predicting emotional states

Table 8. Comparison of classification accuracies illustrating significant advancements and the superior performance of our current model

No.	Reference	Year of Publication	Accuracy
1	[35]	2019	76%
2	[33]	2020	78.3%
4	[18]	2020	96.77%
5	[26]	2023	97.20%
6	**Our work**	**2024**	**98.40%**

7. Conclusion

This study's comprehensive exploration of electrochemical-based EEG brain signal recognition using deep learning techniques has culminated in the development of a robust model that achieves a classification accuracy of 98.4% on the SEED database. Our findings underscore the model's capability to interpret complex neurological data effectively, facilitating advancements in both theoretical and applied neuroscience. Given the model's high accuracy and efficiency, we recommend its integration into clinical diagnostic processes, particularly for conditions that involve nuanced emotional assessments such as depression or anxiety disorders. Developers should consider implementing this model within real-time monitoring systems for patients with neurological disorders, providing ongoing, dynamic insights into patients' emotional states that can enhance therapeutic outcomes. Further collaboration between neuroscientists, psychologists, and AI specialists is recommended to refine the model's applications, ensuring it meets the varied needs across different fields such as cognitive science and psychiatric research. Future studies should include a broader array of EEG datasets, including those with more diverse demographic backgrounds and varying emotional states, to test the model's generalizability and robustness across different populations. Investigating alternative neural network architectures or advanced optimization algorithms might yield improvements in model efficiency and performance, particularly in minimizing false positives and negatives. There is a potential to enhance model accuracy further by exploring more sophisticated feature extraction techniques that could provide deeper insights into the subtle nuances of EEG signals. Developing interdisciplinary models that incorporate cognitive and physiological parameters could provide a more holistic understanding of brain functions and emotional responses. As AI continues to intersect more with healthcare and personal data, it's crucial to prioritize ethical considerations and privacy in future models to protect patient information. By addressing these recommendations and exploring the suggested avenues for future research, the field can continue to advance our understanding and capabilities in using artificial intelligence for EEG signal analysis and brain function interpretation.

Declaration

Conflict of Interest: The authors declare that they have not received any support from any organization for the submitted work. Furthermore, there are no known competing financial or proprietary interests that could have influenced the work reported in this paper.

Dataset Permission

The SEED dataset used in this study was obtained with permission from the SEED manager at the Department of Computer Science, Shanghai Jiao Tong University, Dongchuan Road, Minhang District, Shanghai, China 200240. For further inquiries or to request access to the dataset, please contact seed2022@sjtu.edu.cn.

Code Availability

The code used in this study is available to anyone interested in further developing the work, following correspondence with at least the first and second authors.

8. Acknowledgment
We extend our deepest gratitude to Mohammed Mehany, Wael Hassan, and Zainab Shawa for their insightful comments on this paper. Their expertise in pharmacy, mathematical logic, and software engineering, respectively, significantly enhanced the quality of this work.

9. References

[1] Fei Wu, Ping Yu, Mao L., New Opportunities of Electrochemistry for Monitoring, Modulating, and Mimicking the Brain Signals, JACS Au 2023; 3 (8), 2062-2072 Doi: 10.1021/jacsau.3c00220.

[2] Reyes A. D., Neuronal Signals Thoroughly Recorded. Nature 2019; 575 (7781), 38−39.

[3] Hill CL., Stephens G.J. An Introduction to Patch Clamp Recording. Methods Mol Biol. 2021; 2188:1-19. Doi: 10.1007/978-1-0716-0818-0_1. PMID: 33119844.

[4] Zhang X., Ma Z., Zheng H., Li T., Chen K., Wang X., Liu C., Xu L., Wu X., Lin D., et al. The combination of brain–computer interfaces and artificial intelligence: Applications and challenges. Ann. Transl. Med. 2020; 8:712. Doi: 10.21037/atm.2019.11.109. - DOI - PMC - PubMed.

[5] Tsuboi D., Nagai T., Yoshimoto J., Kaibuchi K. (2024). Neuromodulator regulation and emotions: insights from the crosstalk of cell signaling. Front. Mol. Neurosci. 17:1376762. Doi: 10.3389/fnmol.2024.1376762 - DOI - PMC - PubMed.

[6] Sörnmo L., Laguna P., Chapter 2 - The Electroencephalogram -A Brief Background, Editor(s): Leif Sörnmo, Pablo Laguna, In Biomedical Engineering, Bioelectrical Signal Processing in Cardiac and Neurological Applications, Academic Press, 2005, Pages 25-53, ISBN 9780124375529, https://doi.org/10.1016/B978-012437552-9/50002-7.

[7] Maffei M.E. 5-Hydroxytryptophan (5-HTP): Natural Occurrence, Analysis, Biosynthesis, Biotechnology, Physiology and Toxicology. Int. J. Mol. Sci. 2021; 22:181. Doi: 10.3390/ijms22010181. - DOI - PMC - PubMed.

[8] Sumi-Ichinose C., Ichinose H., Takahashi E., Hori T., Nagatsu T., Molecular cloning of genomic DNA and chromosomal assignment of the gene for human aromatic L-amino acid decarboxylase, the enzyme for catecholamine and serotonin biosynthesis. Biochemistry. 1992 Mar 3;31(8):2229-38. doi: 10.1021/bi00123a004. PMID: 1540578.

[9] Bamalan O.A., Moore M.J., Al Khalili Y., Physiology, Serotonin. [Updated 2023 Jul 30]. In: StatPearls [Internet]. Treasure Island (FL): StatPearls Publishing; 2024 Jan-. Available from: https://www.ncbi.nlm.nih.gov/books/NBK545168/

[10] Lin S.H., Lee L.T., Yang Y.K., Serotonin and mental disorders: a concise review on molecular neuroimaging evidence. Clin Psychopharmacol Neurosci. 2014 Dec;12(3):196-202. Doi: 10.9758/cpn.2014.12.3.196. Epub 2014 Dec 26. PMID: 25598822; PMCID: PMC4293164.

[11] Lovinger D.M., Communication networks in the brain: neurons, receptors, neurotransmitters, and alcohol. Alcohol Res Health. 2008;31(3):196-214. PMID: 23584863; PMCID: PMC3860493.

[12] Hosseini E., Brain-to-brain communication: the possible role of brain electromagnetic fields (As a Potential Hypothesis). Heliyon. 2021 Mar 1;7(3): e06363. Doi: 10.1016/j.heliyon. 2021.e06363. PMID: 33732922; PMCID: PMC7937662.

[13] Ahmad I., Ansari F., Dey U., (2020). A Review of EEG Recording Techniques. International Journal of Electronics and Communication Engineering & Technology (IJECET), Volume 3, pp.177-186.

[14] Beres A. M., Time is of the Essence: A Review of Electroencephalography (EEG) and Event-Related Brain Potentials (ERPs) in Language Research. Appl Psychophysiol Biofeedback. 2017 Dec;42(4):247-255. doi: 10.1007/s10484-017-9371-3. PMID: 28698970; PMCID: PMC5693972.

[15] Saeidi M., Karwowski W., Farahani F.V., Fiok K., Taiar R., Hancock P.A., Al-Juaid A., Neural Decoding of EEG Signals with Machine Learning: A Systematic Review. Brain Sci. 2021 Nov 18;11(11):1525. Doi: 10.3390/brainsci11111525. PMID: 34827524; PMCID: PMC8615531.

[16] Marco Vilela, Leigh R. Hochberg, Chapter 8 - Applications of brain-computer interfaces to the control of robotic and prosthetic arms, Editor(s): Nick F. Ramsey, José del R. Millán, Handbook of Clinical Neurology, Elsevier, Volume 168, 2020, Pages 87-99, ISSN 0072-9752, ISBN 9780444639349, https://doi.org/10.1016/B978-0-444-63934-9.00008-1.

[17] Erat, K., Şahin, E.B., Doğan, F. et al. Emotion recognition with EEG-based brain-computer interfaces: a systematic literature review. Multimed Tools Appl (2024). https://doi.org/10.1007/s11042-024-18259-z.

[18] Liu J., Wu G., Luo Y., Qiu S., Yang S., Li W. and Bi Y., (2020) EEG-Based Emotion Classification Using a Deep Neural Network and Sparse Autoencoder. Front. Syst. Neurosci. 14:43. Doi: 10.3389/fnsys.2020.00043.

[19] Huang X., Wang S.-J., Liu X., Zhao G., Feng X., Pietikainen, M. Discriminative spatiotemporal local binary pattern with revisited integral projection for spontaneous facial micro-expression recognition. IEEE Trans.

Affect. Comput. 2017, 10, 32–47. [CrossRef]

[20] Petrushin V., Emotion in speech: Recognition and application to call centers. Artif. Neural Netw. Eng. 1999, 710, 22.

[21] Yan J., Zheng W., Xin M., Yan J., Integrating facial expression and body gesture in videos for emotion recognition. IEICE Trans. Inf. Syst. 2014, 97, 610–613. [CrossRef]

[22] Katsigiannis S., Ramzan N., DREAMER: A database for emotion recognition through EEG and ECG signals from wireless low-cost off-the-shelf devices. IEEE J. Biomed. Health Inform. 2017, 22, 98–107. [CrossRef] [PubMed].

[23] Huang Z., Ma Y., Wang R., Li W., Dai Y., A Model for EEG-Based Emotion Recognition: CNN-Bi-LSTM with Attention Mechanism. Electronics 2023, 12, 3188. https://doi.org/10.3390/ electronics12143188.

[24] Li T, Liu W, Zheng W, Lu B (2019) Classification of five emotions from EEG and eye movement signals: discrimination ability and stability over time. In: 2019 9th international IEEE/EMBS conference on neural engineering (NER), San Francisco, CA, USA.

[25] Choi H., Park J., Yang Y.-M., A Novel Quick-Response Eigenface Analysis Scheme for Brain–Computer Interfaces. Sensors 2022, 22, 5860. [CrossRef]

[26] Ju X., Li M., Tian, W. et al., EEG-based emotion recognition using a temporal-difference minimizing neural network. Cogn Neurodyn 18, 405–416 (2024). https://doi.org/10.1007/s11571-023-10004-w.

[27] J. Atkinson and D. Campos, Improving BCI-based emotion recognition by combining EEG feature selection and kernel classifiers, Expert Syst. Appl., vol. 47, pp. 35–41, Apr. 2016.

[28] N. Kumar, K. Khaund, and S. M. Hazarika, Bispectral analysis of EEG for emotion recognition, in Proc. 7th Int. Conf. Intell. Human Comput. Interact. (IHCI), Allahabad, India, 2015, pp. 31–35.

[29] S. Wang, Y. Zhu, L. Yue, and Q. Ji, Emotion recognition with the help of privileged information, IEEE Trans. Auton. Mental Develop., vol. 7, no. 3, pp. 189–200, Sep. 2015.

[30] M. Stikic, R. R. Johnson, V. Tan, and C. Berka, EEG-based classification of positive and negative affective states, Brain Comput. Interfaces, vol. 1, no. 2, pp. 99–112, 2014.

[31] S. Nasehi and H. Pourghassem, An optimal EEG-based emotion recognition algorithm using Gabor features, WSEAS Trans. Signal Process., vol. 8, no. 3, pp. 87–99, 2012.

[32] V. Gupta, M. D. Chopda, and R. B. Pachori, Cross-subject emotion recognition using flexible analytic wavelet transform from EEG signals, IEEE Sensors J., vol. 19, no. 6, pp. 2266–2274, Mar. 2019.

[33] Cimtay, Y.; Ekmekcioglu, E. Investigating the use of pretrained convolutional neural network on cross-subject and cross-dataset EEG emotion recognition. Sensors 2020, 20, 2034. [CrossRef].

[34] Wang Y, Huang Z, McCane B, Neo P (2018) EmotioNet: a 3-D convolutional neural network for EEG-based emotion recognition. In: 2018 international joint conference on neural networks (IJCNN), Rio de Janeiro, Brazil.

[35] Thejaswini, S.; Ravikumar, K.M.; Jhenkar, L.; Natraj, A.; Abhay, K.K. Analysis of EEG based emotion detection for DEAP and SEED-IV databases using SVM 208 II. Lit. Rev. 2019, 1, 207–211.

[36] Al-Nafjan A., Hosny M., Al-Ohali Y., and Al-Wabil A., Review and classification of emotion recognition based on EEG brain-computer interface system research: A systematic review," Appl. Sci., vol. 7, no. 12, pp. 1–34, 2017.

[37] Alarcão S. M., Fonseca M. J., Emotions recognition using EEG signals: A survey, 2019 IEEE Trans. Affective Comput., vol. 10, no. 3, pp. 374–393.

[38] Issa S., Peng Q., You X., Emotion Classification Using EEG Brain Signals and the Broad Learning System, 2020; IEEE Transactions on Systems, Man, and Cybernetics: Systems. PP. 1-10. 10.1109/TSMC.2020.2969686.

[39] Lovinger D.M., Communication networks in the brain: neurons, receptors, neurotransmitters, and alcohol. Alcohol Res Health. 2008;31(3):196-214. PMID: 23584863; PMCID: PMC3860493.

[40] Pivovarov A.S., Calahorro F., Walker R.J., Na+/K+-pump and neurotransmitter membrane receptors. Invert Neurosci. 2018 Nov 28;19(1):1. Doi: 10.1007/s10158-018-0221-7. PMID: 30488358; PMCID: PMC6267510.

[41] Grider M.H., Jessu R., Kabir R., Physiology, Action Potential. [Updated 2023 May 8]. In: StatPearls [Internet]. Treasure Island (FL): StatPearls Publishing; 2024 Jan-. Available from: https://www.ncbi.nlm.nih.gov/books/NBK538143/

[42] Südhof T.C., Calcium control of neurotransmitter release. Cold Spring Harb Perspect Biol. 2012 Jan 1;4(1): a011353. Doi: 10.1101/cshperspect. a011353. PMID: 22068972; PMCID: PMC3249630.

[43] Purves D., Augustine G.J., Fitzpatrick D., et al., editors. Neuroscience. 2nd edition. Sunderland (MA): Sinauer Associates; 2001. Excitatory and Inhibitory Postsynaptic Potentials. Available from:

https://www.ncbi.nlm.nih.gov/books/NBK11117/.

[44] Postnova S, Rosa E., & Braun H., 2010; Neurones and Synapses for Systemic Models of Psychiatric Disorders. Pharmacopsychiatry. 43 Suppl 1. S82-91. 10.1055/s-0030-1252025.

[45] R. P. "Prof. Walter Nernst, For. Mem. R.S." Nature, 149;3779(1942):375-376.

[46] Otero T.F., 2022; Exploring Brain Information Storage/Reading for Neuronal Connectivity Using Macromolecular Electrochemical Sensing Motors. Adv. Intell. Syst.,4:2100058. https://doi.org/10.1002/aisy.202100058.

[47] Dfarhud D, Malmir M, Khanahmadi M., Happiness & Health: The Biological Factors- Systematic Review Article. Iran J Public Health. 2014; 43(11):1468-77. PMID: 26060713; PMCID: PMC4449495.

[48] Li Y., Li L., Stephens M.J., Zenner D., Murray K.C., Winship I.R., Vavrek R., Baker G.B., Fouad K., Bennett D.J., Synthesis, transport, and metabolism of serotonin formed from exogenously applied 5-HTP after spinal cord injury in rats. J Neurophysiol. 2014 Jan;111(1):145-63. doi: 10.1152/jn.00508.2013. Epub 2013 Sep 25. PMID: 24068759; PMCID: PMC3921369.

[49] Mine M., Mizuguchi H., Takayanagi T., Kinetic analyses of two-steps oxidation from l-tyrosine to l-dopaquinone with tyrosinase by capillary electrophoresis/dynamic frontal analysis, Analytical Biochemistry, 2022; Volume 655, 114856, ISSN 0003-2697, https://doi.org/10.1016/j.ab.2022.114856.

[50] Daubner S.C., Le T., Wang S., Tyrosine hydroxylase and regulation of dopamine synthesis. Arch Biochem Biophys,2011 ;508(1):1-12. Doi:10.1016/j.abb.2010.12.017. Epub 2010 Dec 19. PMID: 21176768; PMCID: PMC3065393.

[51] Mura A., Jackson D., Manley M.S., Young S.J., Groves P.M., Aromatic L-amino acid decarboxylase immunoreactive cells in the rat striatum: a possible site for the conversion of exogenous L-DOPA to dopamine. Brain Res. 1995;704(1):51-60. Doi: 10.1016/0006-8993(95)01104-8. PMID: 8750961.

[52] Cay M., Ucar C., Senol D., Cevirgen F., Ozbag D., Altay Z., Yildiz S., Effect of increase in cortisol level due to stress in healthy young individuals on dynamic and static balance scores. North Clin Istanb. 2018;5(4):295-301. Doi: 10.14744/nci.2017.42103. PMID: 30859159; PMCID: PMC6371989.

[53] Miller WL, Auchus RJ. The molecular biology, biochemistry, and physiology of human steroidogenesis and its disorders. Endocr Rev. 2011 Feb;32(1):81-151. doi: 10.1210/er.2010-0013. Epub 2010 Nov 4. Erratum in: Endocr Rev. 2011 Aug;32(4):579. PMID: 21051590; PMCID: PMC3365799.

[54] Mou, J.; Ding, J.; Qin, W. Deep Learning-Enhanced Potentiometric Aptasensing with Magneto-Controlled Sensors. Angew C., Int E.d., 2023; 62 (3), No. e202210513.

[55] Pan J., Li Y., Wang J., 2016; An EEG-based brain-computer interface for emotion recognition. In: international joint conference on neural networks (IJCNN), Vancouver, Canada, pp 2063–2067.

[56] Liu Y., Yu M., Zhao G., Song J., Ge Y., Shi Y., 2017; Real-time movie-induced discrete emotion recognition from EEG signals. IEEE Trans Affect Comput 9:550–562.

[57] Goshvarpour A., Goshvarpour A., 2019; EEG spectral powers and source localization in depressing, sad, and fun music videos focusing on gender differences. Cogn Neurodyn 13:161–173.

[58] Moon S.E., Chen C.J., Hsieh C.J., Wang J.L., Lee J.S., 2020; Emotional EEG classification using connectivity features and convolutional neural networks. Neural Netw 132:96–107.

[59] Al-Nafjan A., Hosny M., Al-Ohali Y., Al-Wabil A., 2017; Review and classification of emotion recognition based on EEG brain-computer interface system research: a systematic review. Appl Sci 7:1239.

[60] Alarca˜o S.M., Fonseca M.J., 2019; Emotions recognition using EEG signals: a survey. IEEE Trans Affect Comput 10:374–393.

[61] Torres E.P., Torres E.A., Hernández-Álvarez M., Yoo S.G., 2020; EEG-based BCI emotion recognition: a survey. Sensors 20:5083.

[62] Huang H., Xie Q., Pan J., He Y., Wen Z., Yu R., Li Y., 2021; An EEG-based brain computer interface for emotion recognition and its application in patients with disorder of consciousness. IEEE Trans Affect Comput 12:832–842.

[63] Yu C., Wang M., Survey of emotion recognition methods using EEG information, 2022; Cognitive Robotics, Volume 2, Pages 132-146, ISSN 2667-2413, https://doi.org/10.1016/j.cogr.2022.06.001.

[64] van den Broek, E. L., Ubiquitous emotion-aware computing. Pers, 2013; Ubiquit. Comput. 17, 53–67. Doi: 10.1007/s00779-011-0479-9.

[65] Zheng W.L., and Lu B.L., Investigating critical frequency bands and channels for EEG-based emotion recognition with deep neural networks, 2015; IEEE Trans. Auton. Mental, 162–175. Doi: 10.1109/TAMD.2015.2431497.

[66] Petrantonakis P. C., Hadjileontiadis L. J., Emotion recognition from EEG using higher order crossings, 2010; IEEE Trans. Inform. Technol. Biomed. 14, 186–197. Doi: 10.1109/TITB.2009.2034649.

[67] Light G.A., Williams L.E., Minow F., Sprock J., Rissling A., Sharp R., Swerdlow N.R., Braff D.L., Electroencephalography (EEG) and event-related potentials (ERPs) with human participants. Curr Protoc Neurosci. 2010; Chapter 6: Unit 6.25.1-24. Doi: 10.1002/0471142301.ns0625s52. PMID: 20578033; PMCID: PMC2909037.

[68] Johns Hopkins Medicine (JHM), [Online]. Available: http://www.hopkinsmedicine.org.

[69] Jenke R., Peer A., Buss M., Feature extraction and selection for emotion recognition from EEG, 2014; IEEE Trans. Affective Comput., vol. 5, no. 3, pp. 327–339.

[70] Soleymani M., Pantic M., Pun T., Multimodal emotion recognition in response to videos, in Proc, 2015; Int. Conf. Affect. Comput. Intell. Interact. (ACII). Xi'an, China, pp. 491–497.

[71] Trans Cranial Technologies. [Online]. Available: https://www.trans-cranial.com.

[72] Zheng W.L., Liu W., Lu Y., Lu B.L., Cichocki A., EmotionMeter: A multimodal framework for recognizing human emotions, 2019; IEEE Trans. Cybern., vol. 49, no. 3, pp. 1110–1122.

[73] Bahari F., Janghorbani A., EEG-based emotion recognition using recurrence plot analysis and k nearest neighbor classifier, In 2013 20th Iranian Conference on Biomedical Engineering (ICBME) (Tehran: IEEE), 228–233. Doi: 10.1109/ICBME.2013.6782224.

[74] Orhan U., Hekim M., Ozer M., EEG signals classification using the k-means clustering and a multilayer perceptron neural network model, 2011; Expert Syst. Appl. 38, 13475–13481. Doi: 10.1016/j.eswa.2011.04.149.

[75] Wang Y., Qiu S., Li J., Ma X., Liang Z., Li H., et al., EEGbased emotion recognition with similarity learning network, in 2019 41st Annual International Conference of the IEEE Engineering in Medicine and Biology Society (EMBC) (Berlin: IEEE), 1209–1212. Doi: 10.1109/EMBC.2019. 8857499.

[76] Tripathi S., Acharya S., Sharma R. D., Mittal S., Bhattacharya S., Using deep and convolutional neural networks for accurate emotion classification on deap dataset, 2017; in Proceedings of the Thirty-First AAAI Conference on Artificial Intelligence (Hawaiian, HI), 4746–4752.

[77] Fu Q., Luo Y., Liu J., Bi J., Qiu S., Cao Y., et al, Improving learning algorithm performance for spiking neural networks, in 2017 IEEE 17th International Conference on Communication Technology (ICCT) (Chengdu: IEEE), 1916–1919. Doi: 10.1109/ICCT.2017.8359963.

[78] Liu J., Huang Y., Luo Y., Harkin J., McDaid L., Bio-inspired fault detection circuits based on synapse and spiking neuron models, 2019; Nerocomputing 331, 473–482. Doi: 10.1016/j.neucom.2018.11.078.

[79] Liu J., Mcdaid L. J., Harkin J., Karim S., Johnson A. P., Millard A. G., et al., Exploring self-repair in a coupled spiking astrocyte neural network., 2018a; IEEE Trans. Neural Netw. Learn. Syst. 30, 865–875. Doi: 10.1109/TNNLS.2018.2854291.

[80] Liu J., Sun T., Luo Y., Fu Q., Cao Y., Zhai J., et al.; Financial data forecasting using optimized echo state network, in 2018b 25th International Conference on Neural Information Processing (ICONIP), eds L. Cheng, A. C. S. Leung, and S. Ozawa (Cham: Springer), 138–149. Doi: 10.1007/978-3-030-04221-9_13.

[81] Luo Y., Lu Q., Liu J., Fu Q., Harkin J., McDaid L., et al., Forest fire detection using spiking neural networks, 2018; in Proceedings of the 15th ACM International Conference on Computing Frontiers (New York, NY: ACM), 371–375. Doi: 10.1145/3203217.3203231.

[82] Tripathi S., Acharya S., Sharma R. D., Mittal S., Bhattacharya S., Using deep and convolutional neural networks for accurate emotion classification on deap dataset, 2017; in Proceedings of the Thirty-First AAAI Conference on Artificial Intelligence (Hawaiian, HI), 4746–4752.

[83] Zhang Q., Chen X., Zhan Q., Yang T., Xia S., Respirationbased emotion recognition with deep learning, 2017; Comput. Ind. 92–93, 84–90. doi: 10.1016/j.compind.2017.04.005.

[84] Lecun Y., Bottou L., Bengio Y., Haffner P., "Gradient-based learning applied to document recognition, 1998; Proc. IEEE, vol. 86, no. 11, pp. 2278–2324.

[85] Simonyan K., Zisserman A., Very deep convolutional networks for large-scale image recognition, 2014; [Online]. Available: http://arxiv.org/abs/1409.1556.

[86] Hinton G. et al., Deep neural networks for acoustic modeling in speech recognition: The shared views of four research groups, 2012; IEEE Signal Process. Mag., vol. 29, no. 6, pp. 82–97.

[87] Goodfellow I., Bengio Y., Courville A., Deep Learning. Cambridge, MA, USA: MIT Press, 2016; [Online]. Available: http://www.deeplearningbook.org.

[88] Kingma D.P. Ba J., Adam: A method for stochastic optimization, 2014; arXiv preprint arXiv:1412.6980.